Epoxy Composites Based on Glass Beads. II. Mechanical Properties

N. AMDOUNI, H. SAUTEREAU, and J. F. GERARD*

Laboratoire des Matériaux Macromoléculaires, URA CNRS n° 507, Institut National des Sciences Appliquées de Lyon, 20, Avenue A. Einstein, 69621 Villeurbanne Cedex, France

SYNOPSIS

A DGEBA/DDA network was used to study the toughening effect due to the introduction of glass beads with different volume fractions. The influence of surface treatment was also studied by comparing untreated, silane-treated glass beads, and beads coated with different thicknesses of an elastomeric adduct. The effect of the volume fraction of glass and the surface treatment were discussed in terms of elastic and plastic properties. The results were compared with the usual theoretical models. Linear elastic fracture mechanics and impact tests were performed to study the crack propagation process. The various parameters influenced the deformation mechanism, especially for the coated glass bead composites, for which an optimum thickness was displayed. A large improvement in G_{Ic} value was obtained with a slight decrease for the stiffness. © 1992 John Wiley & Sons, Inc.

INTRODUCTION

Much work has been done on the mechanical behavior of particulate-filled thermoset composites. Much experimental data has been collected on the effect of different parameters, such as the volume fraction or the surface treatment of the particles, shape factor, etc.[1-7] In parallel, many theoretical studies have been developed to describe mechanical properties, especially the elastic modulus, E.

More recently, different ways have been investigated to improve the fracture toughness of thermoset composites. In fact, if the thermal—that is, glass transition temperature, T_g—and elastic mechanical properties of thermoset composites are interesting, in most of the applications a better fracture toughness is required. First, the most widely used method was the addition of a second elastomeric phase in the matrix.[8] This method, applied to particulate composites, leads to hybrid materials[1-3,9-12] with an improved resistance to the crack propagation.[9-12] Such an addition of a low T_g component as a dispersed phase in the thermoset matrix leads to a better fracture toughness, but also to a decrease of the modulus.

In addition, a part of the elastomer, for which a phase separation occurs during curing, remains dissolved in the matrix, which lowers the glass transition temperature of the material.[12]

A second method consists of increasing the filler–matrix adhesion using a coupling agent. In this case, only higher strengths of the particulate composites have been observed and no significant improvement of the fracture toughness was noted.[1-7]

Many theoretical and experimental studies have shown that the insertion of a soft interlayer at the filler–matrix interface led to a tougher composite. Such a method permits improvement of the toughness of the material without any loss of stiffness[13] or thermal properties.[14,15] In fact, theoretical analysis, developed on particulate and fibrous composites,[16-18] has shown that toughness could be maximized by controlling the thickness, and the modulus, of the interlayer. Another method of interest is to coat the rigid particles with a thin layer of elastomer (about 1 to 4% of the radius) to reduce the residual stresses concentrated at the interface during curing of the composite or/and during the shrinkage of the matrix.[16,19] In fact, the thermal expansion coefficients of the matrix and the filler are very different.

* To whom correspondence should be addressed.

Journal of Applied Polymer Science, Vol. 46, 1723–1735 (1992)
 CCC 0021-8995/92/101723-13

Many experimental studies conducted on glass beads,[20-22] carbon,[14,23] or glass fibers[24-26] composites confirm the value of such an approach and the validity of the theoretical micromechanical models.

This work is the second part of a study on the use of a crosslinked elastomer based on a CTBN (carboxy-terminated butadiene acrylonitrile copolymer) reactive rubber as an interphase in glass beads epoxy composites. In the first article,[15] we studied the viscoelastic properties of composites as a function of volume fraction and surface treatment of glass, and elastomeric interphase thickness. The dynamic mechanical spectroscopy allowed us to demonstrate the three phase structure of the composites: filler–interphase–matrix. In addition, the mobility of the macromolecular chains in the vicinity of the glass surface is dependent on the surface treatment. When the glass is treated using a coupling agent (γ-aminopropyltriethoxysilane, γ-APS), the viscoelastic characteristics, especially the apparent activation energy of the main relaxation, α, of the matrix, show that the mobility is reduced. Thus, in this case, an interphase constituted by the epoxy matrix with a reduced mobility is created around the glass beads. On the contrary, for the elastomer coated glass beads composites, the mobility of epoxy chains in the vicinity of the elastomer interphase is increased.

The purpose of this article is to study the mechanical properties of particulate epoxy composites described in the first part.[15] A systematic work was conducted on glass beads/DGEBA-DDA epoxy matrix composites by investigating the elastic and yielding behaviors, and also the fracture properties, using the linear elastic fracture mechanics. Various parameters, such as volume fraction and surface treatment of glass (untreated, silane treated, and elastomer coated), were studied. Special attention was kept on the effect of the elastomer interlayer thickness to compare the experimental data to the trends provided by the theoretical models developed in the literature.

EXPERIMENTAL

Epoxy Matrix

The synthesis and properties of the epoxy matrix of composites was described in previous articles.[27,28] This matrix was based on an epoxy prepolymer DGEBA (diglycidyl ether of bisphenol-A, $\overline{M_n}$ = 380 g, supplied by Bakelite) and the dicyandiamide (Dicy), DDA (Bakelite VE2560). Benzyldimethylamine, BDMA, was used as catalyst and the stoichiometric ratio (amino hydrogen to epoxy) was equal to 0.6. With this chemical system, the cure schedule strongly influences the crosslinking density,[27] due to changes in the reaction pathway with curing temperature. Thus, a single and a well-defined cure schedule was chosen: 1 h at 120°C followed by 1 h at 180°C in rotated, PTFE-coated molds to prevent the Dicy or the glass beads precipitation.

The glass transition temperature of the matrix was about 140°C.

Glass Beads–Surface Treatments

As explained in the first article,[15] glass beads from Sovitec (A050) with particle sizes ranging from 4 to 44 μm were used with three kinds of surface treatments:

- No treatment (noted untreated),
- Silane treated: application of γ-aminopropyltriethoxysilane, γ-APS (A1100 from Union Carbide), and
- Elastomer coated, using a crosslinked adduct with different thickness of rubbery interlayer on the glass surface. The synthesis and application of this elastomer were described in the previous article.[15] e/r ratios (thickness of the elastomeric interlayer to radius of the beads) varied from 0 to 6.5%. The glass transition temperature, T_g, of this soft interlayer was about −55°C.

Composite Materials

Composite materials were made from various volume fractions (from 0 to 30%) of glass beads with the various surface treatments. The influence of the interlayer thickness was studied on composite materials with the same filler content (20% vol).

Mechanical Tests on the Epoxy–Glass Beads Composites

Young's moduli (E) were obtained from a tensile test at room temperature on an Adamel–Lhomargy (DY25) tensile machine, equipped with an EX10 extensometer (strain rate: $3.3 \times 10^{-4}\ s^{-1}$).

Two kinds of compression tests were performed to obtain the preyielding and yielding behaviors. In the preyield stage, the non elastic, work-hardening rate, K, was measured during compression tests made at a constant rate ($\dot{\epsilon} = 2 \times 10^{-4}\ s^{-1}$) on cylindrical specimens (9.2 mm long and 5 mm diameter).

As described in previous articles,[29,30] K is a measure of the resistance of the material to develop plastic strain. The composite materials were compared using the ratio K/M (M: compression modulus) to take into account the changes in the stiffness.

The yield stress, σ_y, was determined from compression tests at a strain rate of 8.3×10^{-4} s^{-1} on parallelepipedic specimens ($20 \times 10 \times 6$ mm^3).

Impact strength measurements were performed on an instrumented Charpy pendulum (velocity of the stricker: 3 $m \cdot s^{-1}$) on unnotched specimens ($60 \times 10 \times 6$ mm^3) with a span-to-length equal to 40 mm. The total energy at break per unit area (R_S, resilience) and the energy of initiation W_i (work done to reach the maximum load) were recorded.

Single-edge notched specimens (SEN) (thickness, t, about 6 mm and width, ω, about 12 mm, span-to-length: 48 mm) were used for the linear elastic fracture mechanics (LEFM). Cracks of various lengths were machined with a diamond saw and achieved using a razor blade at a temperature about T_g of the epoxy matrix (about 130°C). The fracture toughness, K_{Ic}, and the fracture energy, G_{Ic}, in plane strain conditions were computed from the critical stress for crack propagation and a form factor previously described.[31]

The deformation and the fracture processes were analyzed by scanning electron microscopy (SEM) on the fracture surface of the SEN specimens. A Jeol 840A microscope, operating at 15 kV, was used.

RESULTS AND DISCUSSION

The effect of the different parameters, such as the volume fraction of glass beads with different surface treatments and the thickness of the soft interlayer, are discussed for each behavior: elastic, preyielding, yielding, and fracture properties.

Elastic Mechanical Properties

The values of the Young's modulus at room temperature, E, obtained from tensile tests for the various composite materials, are reported in Tables I and II. The evolution of E as a function of the volume fraction, ϕ_g, of glass beads for the three different surface treatments (untreated, silane treated, and elastomer coated) is represented in Figure 1. In agreement with many studies,[2,5,6,10,32] the Young's modulus increased with increasing ϕ_g. For the same volume fraction of glass beads, the composite prepared from silane treated glass beads exhibits a slightly higher modulus than for untreated or elastomer coated glass particles (Tables I and II). As demonstrated by different workers,[4,5,7,10] the effect of the interfacial bonding, promoted by the γ-APS treatment of glass, does not affect the Young's modulus because the bonding was measured at a low level of strain.

Much work has been performed on the simulation of the modulus of particulate composite materials. Some of this work has been applied to our systems, for example, Eilers,[33] Kerner,[34] Halpin and Kardos,[35] Ishai and Cohen,[36] and Hashin and Shtrickman.[37] For all the models tested, the level of the stress transfer (adhesion) at the matrix–filler interface was not taken into account. Other models may be used and were recently reviewed.[38,39] The results, presented in Figure 1, show that in this composition range, that is, ϕ_g lower than 0.3, most of the models yield the same trends.[3] Nevertheless, it can be observed, as already mentioned,[10] that the data fall close to the lower bound of Ishai and Coh-

Table I Mechanical Characteristics at Room Temperature

Material	Tension E (GPa) (a)	Preyielding K/M (b)	Yielding σ_y (MPa) (c)	Yielding e_y (%)
Epoxy matrix	2.9	0.57	108	6
10% vol untreated	3.65	0.72	113	4.5
20% vol untreated	4.8	0.98	119	4.5
30% vol untreated	6	1.22	128	4
10% vol silane treated	3.5	—	115.5	4.8
20% vol silane treated	4.6	1.23	125.5	4.5
30% vol silane treated	5.6	—	136	4.4

(a) Young's moduli (E), (b) ratio of non-elastic work hardening rate to compressing modulus and (c) yield stresses (σ_y) of composite materials, based on different vol fractions of untreated and silane treated glass beads.

Table II Mechanical Characteristics at Room Temperature of Composite Materials Based on Glass Beads Coated with Various Thickness of Elastomer e/r

Material	Interlayer Thickness e/r (%)	Tension E (GPa)	Preyielding K/M	Yielding σ_y (MPa)	Yielding e_y (%)
20% vol untreated	0	4.8	0.98	119	4.5
20% vol coated	2	4.6	1.02	118	4.5
20% vol coated	2.8	4.55	0.91	118	4.5
20% vol coated	4.2	4.45	0.91	116	4.7
20% vol coated	6.5	4.35	0.74	113	4.8
10% vol coated	4.2	3.45	—	110	5.1
30% vol coated	4.2	5.4	—	123	4.5

en's model,[36] showing that the deformation takes place through a uniform displacement at the particle–matrix interface.

For coated glass beads composites, a slight decrease of the Young's modulus, E, was observed as the soft interlayer thickness increased for the same volume fraction of glass (20% vol, Table II). Even for a ratio thickness of the interphase-to-radius of the particles over 6.5%, a decrease for E about 10% was observed. This behavior cannot be described by such two-phase models, but these trends are in agreement with the theoretical studies developed by Matonis and Small[13] and Broutman and Agarwal.[16]

On the whole, the Young's modulus data show that the elastic mechanical behavior is not greatly influenced by the surface treatment of glass beads.

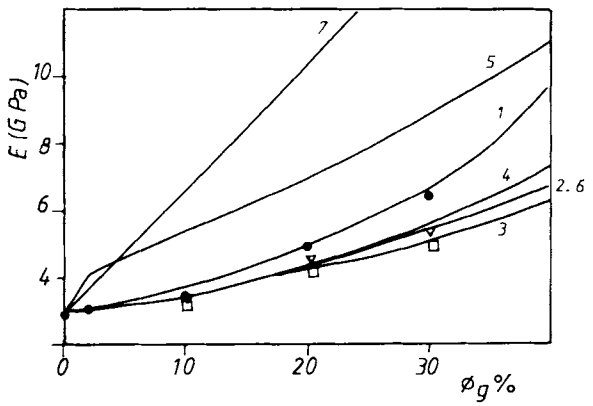

Figure 1 Young's modulus vs. the vol fraction of glass beads. (▽) untreated glass, (●) silane treated, and (■) elastomer coated (e/r = 4.2%). Simulation of the Young's modulus using various models of the literature. (1) Eilers, (2) Kerner, (3) Halpin-Tsaï, (4) and (5) lower and higher bounds of the Ishai–Cohen model, respectively, and (6) and (7) lower and higher bounds of Hashin–Shtrickman model.

We have shown that it is possible to introduce a thin elastomeric interlayer at the glass–epoxy interface without a large decrease in the stiffness of the composite materials.

Preyielding and Yielding Properties of Composites

All of the composite materials display, in uniaxial compression, a ductile behavior with the existence of plastic deformation. Tables I and II give the values obtained in the preyield stage during compression tests at a constant strain rate for the nonelastic work hardening rate, K, expressed as K/M ratio (work hardening rate-to-compression modulus, M). Figure 2 displays the evolution of the K/M and yield stress, σ_y, with the volume fraction of glass particles. As the volume fraction of glass increases, these two characteristics also increase. According to the me-

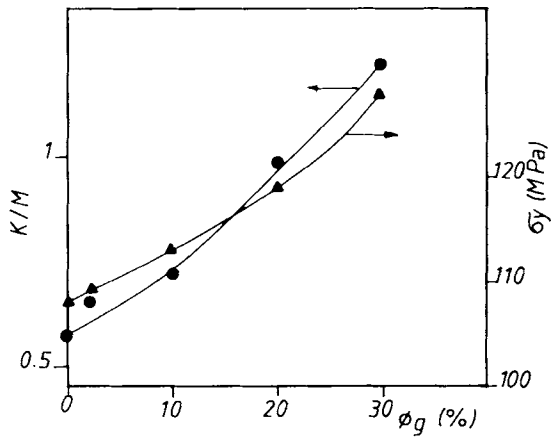

Figure 2 Evolution of the ratio of nonelastic work hardening rate, K, to compression modulus, M, and yield stress, σ_y, as a function of the vol fraction of glass beads (untreated).

Table III Fracture Properties and Charpy Impact Characteristics at Room Temperature of Composite Materials Based on Different Vol Fractions of Untreated and Silane Treated Glass Beads

	Charpy Test		LEFM	
Material	R_S (kJ m^{-2})	W_i (%)	K_{Ic} (MPa m$^{-1/2}$)	G_{Ic} (kJ m^{-2})
Epoxy matrix	17 ± 1.9	6.2 ± 2.6	1.6	0.75
10% vol untreated	11.7 ± 1	54 ± 2.5	1.78	0.77
20% vol untreated	10.4 ± 1.2	48 ± 4	1.88	0.67
30% vol untreated	9.6 ± 1.6	45 ± 4	2.02	0.62
10% vol silane treated	14.6 ± 0.9	58 ± 2	1.7	0.74
20% vol silane treated	12.6 ± 0.7	54 ± 3	1.8	0.63
30% vol silane treated	12.5 ± 1.5	52 ± 3	1.9	0.61

tallurgical approach described in previous articles,[29,30] K/M varies as the inverse of the defect nucleation rate and is greatly influenced by any change in the mesostructure of the material. Thus, the capacity for nucleation and propagation of defects is reduced by the introduction of untreated glass beads in the epoxy matrix. As the volume fraction of glass particles increases, the interparticle distance decreases and the interactions between triaxial stress fields becomes more important, leading to a decrease in the nucleation of defects.

The yield stress, σ_y, increases with increasing the volume fraction of glass beads in agreement with the literature.[10,40,41] According to many authors, a value of 100 MPa for σ_y seems to be the limit on which the propagation of the plastic deformation becomes more difficult, as observed in our case.

For the same volume fraction of glass bead (20% vol), the silane treatment increases the K/M and σ_y values (Table I). The aminosilane improves the adhesion between phases and, as a result, leads to a better transfer of the local stresses. Thus, the local stress fields are more interconnected. The increasing of local stresses around glass beads is contrary to the development of the nucleation of defects.

It is well known that the underlying mechanism of plastic deformation in particulate-filled epoxies is shear yielding in the matrix.[10] Therefore, the increase in the σ_y value for γ-APS treated glass beads demonstrates that the improvement of stress transfer at the interface induces a larger shear yielding in the epoxy matrix.

In opposition to the silane treatment, the coating of the glass beads with a thin elastomeric interlayer (from 0 to 2.8%) decreases the K/M ratio and slightly affects the yield stress (Table II). The elastomeric interlayer modifies the stress field around particles, as previously mentioned by various theoretical studies.[13,17,18]

The effect of the thickness of the rubbery interlayer on the preyield stage (K/M) is more pronounced than on the yield stress, σ_y (Table III, Fig. 3). This phenomenon was discussed in detail in a previous article.[42] The most important results are that: (1) the effect of the interlayer thickness acts on the initiation of the plastic deformation mechanisms, and (2) the work-hardening rate is constant for e/r lower than 2% and displays a decrease (about 10%) for higher e/r. Since the higher the K value, the less the material is able to deform plastically, such a decrease of K/M value indicates that the composites with the highest interlayer thickness are able to undergo more plastic deformation.

The change of K/M value at an interlayer thickness of between 2% and 2.8% can be explained by

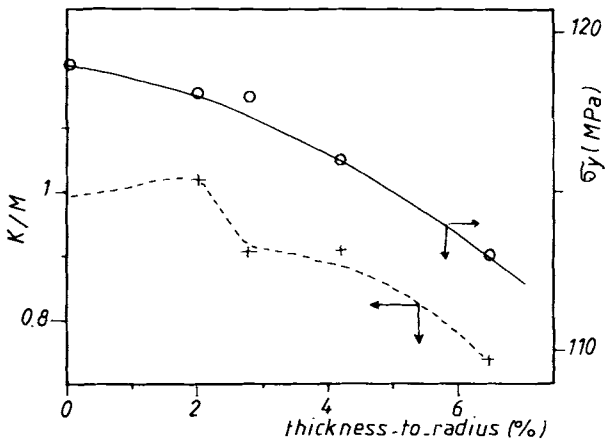

Figure 3 K/M ratio and yield stress, σ_y, vs. the interlayer thickness for coated glass beads composites (20% vol fraction of glass).

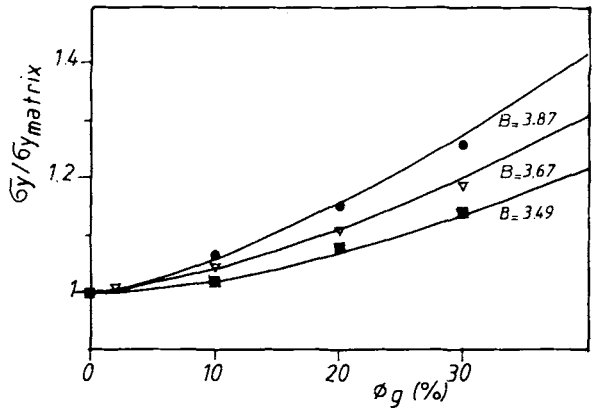

Figure 4 Normalized yield stress, $\sigma_y/\sigma_{y_{matrix}}$, vs. the vol fraction of glass beads (same symbols as in Fig. 1). (——) Turcsanyi's model computed for various values of the B parameter.

the micromechanical analysis made by Ricco et al.[17,18] This theoretical model describes the craze initiation or the shear yielding factors for an elementary model considering a two phase particle imbedded in an infinite matrix under a uniform uniaxial tension. These authors found that for a thickness-to-radius ratio of about 4.2%, the shear yielding is located either at the pole or at the equator of the particle. Thus, for this thickness, an optimum of mechanical properties is also displayed. In our case, the plastic deformation mechanism changes for a lower thickness (about 2.8%). Unfortunately, the assumptions made in the model are not verified: (1) the ratios of the moduli of the interphase and the matrix are not the same (about 1000 in Ricco's model and 6000 in our case), (2) the component occluded in the particle is not the matrix, but glass, (3) the model does not take into account the interactions between the stress fields induced by the different particles, (4) the two-phase particle in the matrix is submitted to a uniform uniaxial tension, and (5) the adhesion between phases is supposed to be perfect and the components are assumed to display an elastic behavior. All these differences have could explained the discrepancy between the calculations and our experimental data. Nevertheless, the critical thicknesses (e/r) are in the same order of magnitude.

Some authors proposed theoretical models to described the evolution of yield stress with volume fraction of particles. Recently, Turcsanyi[43] modified the model developed by Nicolais and Narkis.[44]

The yield stress for the particulate composites can be expressed as:

$$\sigma_y = (1 - \phi_g)(\sigma_{y_{mat}} \exp[B\phi_g])/(1 + 2.5\phi_g)$$

where $\sigma_{y_{mat}}$ is the yield stress of the unfilled matrix. B is a parameter, which could be related to the adhesion between the glass and the epoxy matrix. This model is applied for the various surface treatments of glass (untreated, silane treated, and elastomer coated, e/r = 4.2%, Fig. 4). The B values reported correspond to the best fitting and are in the same range than those reported by Turcsanyi.[42] As expected, when the adhesion is improved by a surface treatment using a silane, B increases in comparison with the untreated glass beads composites. The lower value of B for the elastomer coated glass beads cannot be explained in terms of adhesion. In fact, we showed previously that the introduction of a soft interlayer induces changes of the stress fields.

As displayed in Figure 4, the evolution of the yield

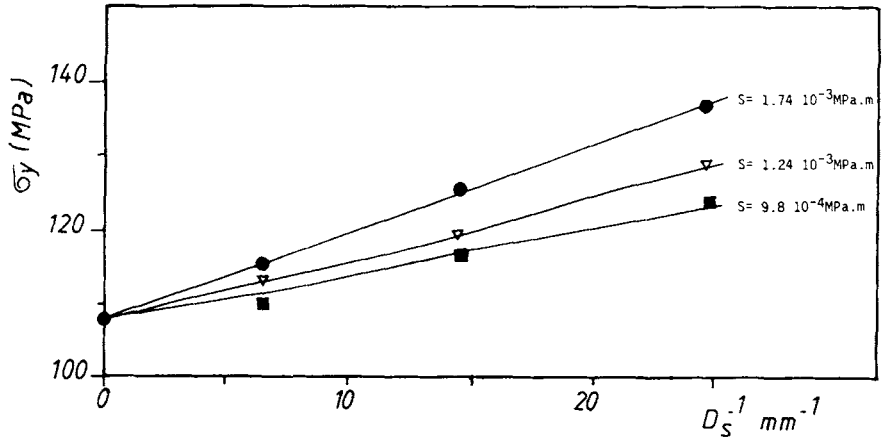

Figure 5 Yield stress, σ_y, vs. the average interparticle distance, $\overline{D_S^{-1}}$, for the different composites: (same symbols as in Fig. 1).

Table IV Charpy Impact Characteristics and Fracture Properties at Room Temperature of Composite Materials Based on Glass Beads Coated with Various Thickness of Elastomer (*e/r*)

		Charpy Test		LEFM	
Material	Interlayer Thickness e/r (%)	R_S (kJ m^{-2})	W_i (%)	K_{Ic} (MPa m$^{-1/2}$)	G_{Ic} (kJ m^{-2})
20% vol untreated	0	10.4 ± 1.2	48 ± 4	1.88	0.67
20% vol coated	2	11.2 ± 2.6	48.5 ± 5	1.92	0.72
20% vol coated	2.8	11.5 ± 1.9	49 ± 7	2.3	1.1
20% vol coated	4.2	12.3 ± 3	52 ± 8	2.15	0.93
20% vol coated	6.5	15 ± 3.3	60.5 ± 6	1.95	0.79
10% vol coated	4.2	12.9 ± 2.5	54 ± 4	1.88	0.91
30% vol coated	4.2	10.9 ± 2	50 ± 4.6	2.11	0.75

stress is close to a linear relationship (at a constant strain rate), as previously described.[40]

Young and Beaumont[45] also proposed a relation for σ_y with the average interparticle distance D_S:

$$\sigma_y = \sigma_{y_{mat}} + S/D_S$$

where S is a constant. D_S can be expressed as:

$$D_S = 2d(1 - \phi_g)/3\phi_g$$

where d is the average diameter of particles.

As shown in Figure 5, a good fitting could be obtained for each surface treatment of glass beads, confirming the effect of the interparticle distance—that is, the interactions between the stress fields around the particles—on the mechanism of the propagation of the plasticity defects.

Fracture Properties of Composites

The fracture properties, obtained from Charpy impact tests, are given in Tables III, IV, and in Figure 6. The total energy at break per area unit (i.e., the resilience, R_S) and the initiation energy, W_i, are reported.

R_S and W_i decrease with increasing the volume fraction, ϕ_g, of the glass beads for the various surface treatments in agreement with the other studies.[4,5,38,46] As noted by Briggs,[38] no theoretical relationship between the characteristics of the components and the concentration can be used to predict the impact strength of filled polymers.

The effect of ϕ_g on the impact properties could be explained by the increase of the stress concentrations at the filler–matrix interface, leading to a more easy initiation of the cracks, as observed on the W_i evolution for the highest volume fractions (Fig. 6). As previously mentioned, the ability of plastic deformation—that is, the propagation of defects—decreases with increasing the volume fraction of particles. As a consequence, the energy absorbed for yielding decreases and contributes to a lower resilience.

In agreement with other studies,[5,46,47] the treatment of a glass surface by a coupling agent slightly improves the unnotched Charpy impact strength (Table III). The impact fracture involves two stages:

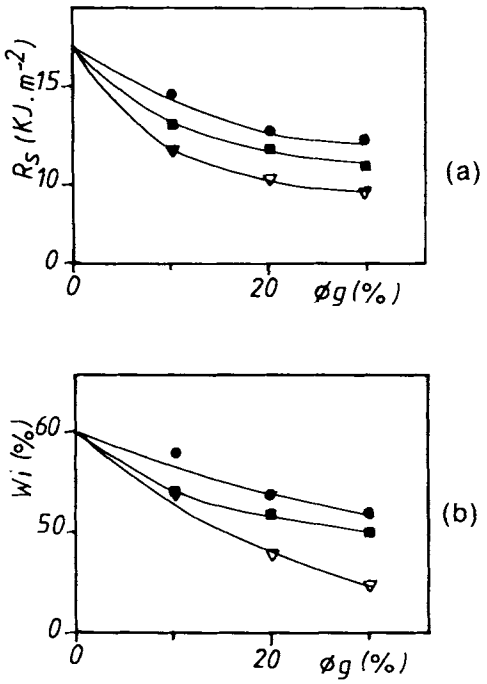

Figure 6 Charpy impact test. Evolution of the energy at break, R_S, (a) and the energy of initiation, W_i, (b) as a function of the volume fraction of glass beads (same symbols as in Fig. 1).

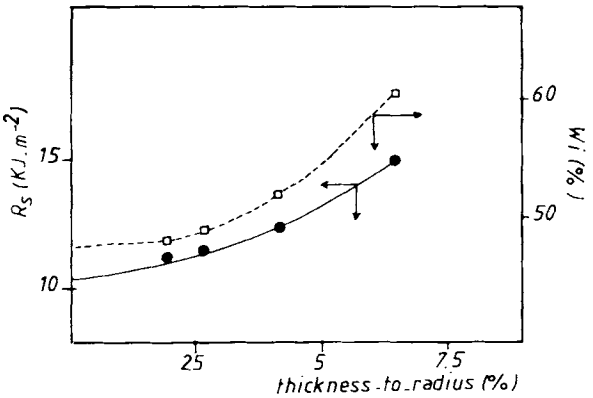

Figure 7 Charpy impact test. Evolution of the energy at break, R_S, and the energy of initiation, W_i, as a function of the elastomer coating thickness e/r (composites with 20% vol fraction of glass).

the initiation and the propagation of cracks. A better adhesion between the filler and the epoxy matrix through the aminosilane leads to a better stress transfer and can delay the initiation of cracks at the interface, in agreement with the observed increasing of the initiation energy (Table III). With the introduction of a soft interlayer, the impact properties are enhanced in comparison with the composites, based on untreated glass beads (Table IV and Fig. 6). Nevertheless, these composites display a lower impact strength than the silane treated glass beads composites. As shown in Figure 7, many microcracks are initiated and propagate all around the coated glass particle. This observation confirms the changes of the stress's distribution when a rubbery interphase is introduced. In addition, the increase of the interlayer thickness, e/r, leads to a continuous increase of both the total energy and the initiation energy (Fig. 8).

The increasing ability to deform plastically for coated particles composites could contribute to a better Charpy impact strength through the increase of energy absorbed by the local plastic deformation at the crack tips.

Peiffer et al.,[24,48] on coated short glass fiber epoxy composites, also observed an increase of the Izod impact strength with increasing the latex thickness. However the energy at break, measured on notched specimens, displayed a maximum. In this case, the measured energy does not take into account the initiation of cracks, thus, a direct comparison with this work is difficult.

Using linear elastic fracture mechanics (LEFM), the values of K_{Ic} (critical stress intensity factor) and G_{Ic} (strain energy release rate) are determined

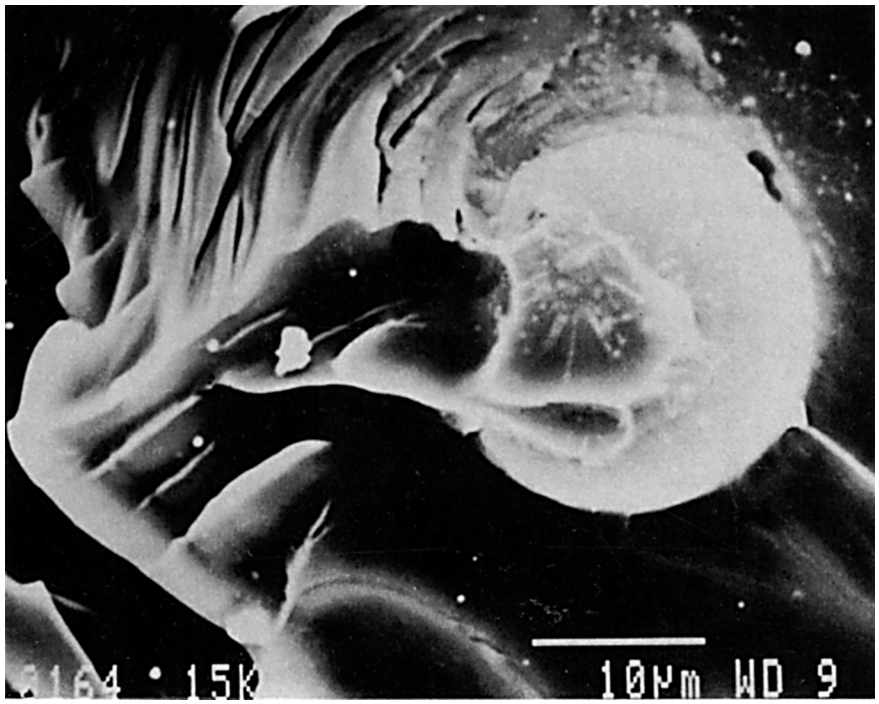

(a)

Figure 8 SEM micrographs of the fracture surfaces of the composites based on: (a) untreated, (b) silane treated, and (c) elastomer coated glass beads (e/r = 4.2%).

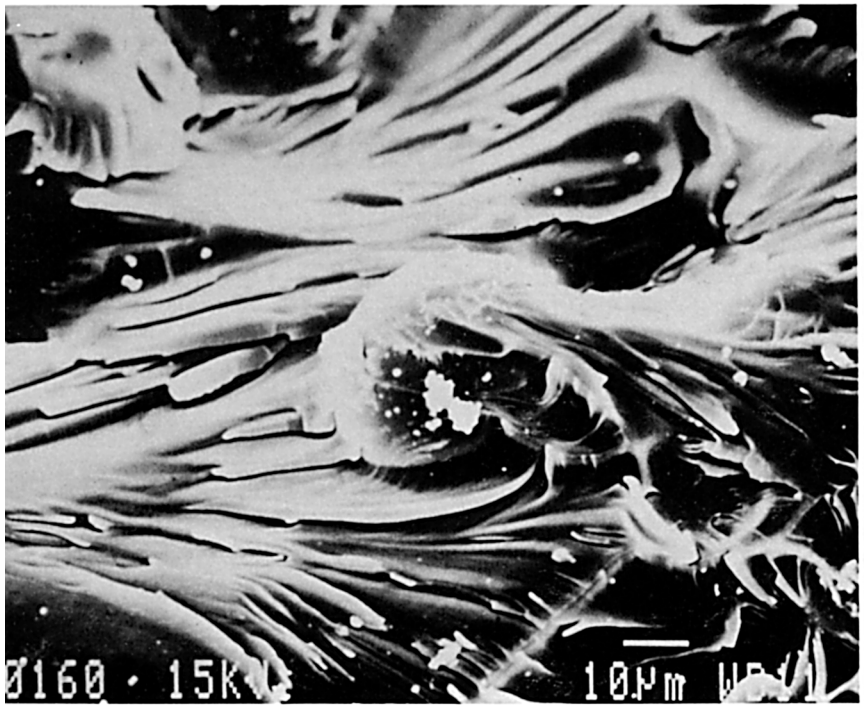

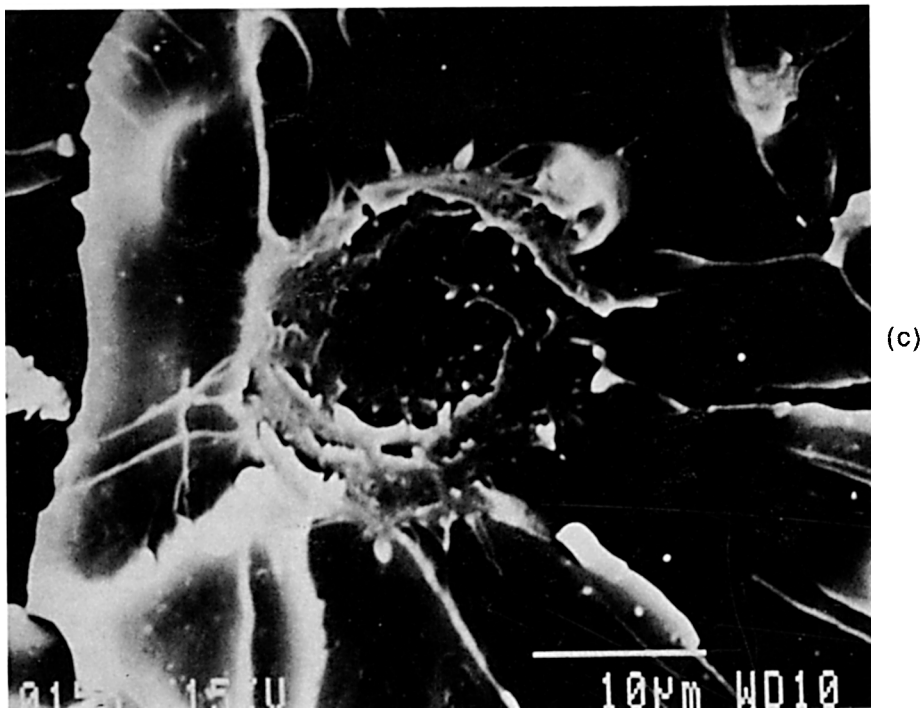

Figure 8 *(Continued from the previous page)*

(Tables III and IV). With the experimental method used in this work, no stick-slip propagation occurs at this temperature and for this strain rate. In agreement with Spanoudakis[7] and Kausch,[2,49] on similar composite materials, K_{Ic} increases linearly with the volume fraction of untreated (or silane treated) glass beads (Fig. 8). In fact, Kausch observed that for high T_g epoxy matrices filled with

glass on silica particles, a stable crack propagation is observed for poorly bonded glass beads and a unstable propagation for well-bonded ones.

The strain energy release rate, G_{Ic}, displays a maximum with the volume fraction, as observed by many workers.[4,7,45,46,49,50] Some of these authors attributed this effect to a change in the fracture mechanisms and other ones to the fact that over 15–20% for the volume fraction, the increase of the modulus is more important than the increase of K_{Ic}.[2]

The toughening mechanisms, reported in the literature, are the crack-pinning and the crack-blunting. In our case, we showed previously that the yield stress, σ_y, for all of the composites is more than 100 MPa, which is a critical value according to Kinloch and Williams.[51] Thus, the crack-blunting mechanism, favored when σ_y is lower than 100 MPa, is probably not the main contribution to the toughening. On the contrary, the presence of tails behind the particles on the fracture surface (Fig. 7) confirms the existence of the crack-pinning mechanism. Some theoretical models have been proposed to describe the crack propagation through rigid particles.[52,53] The theoretical curves and experimental data are compared in Figure 9 in the case of semi-ellipsoïdal secondary microcracks in interaction. In agreement with Spanoudakis,[7] the model assuming the existence of interaction (Evans) fits the data in the range of 0–20%. The discrepancy observed for the highest volume fractions could be explained by the more difficult crack-pinning mechanism.

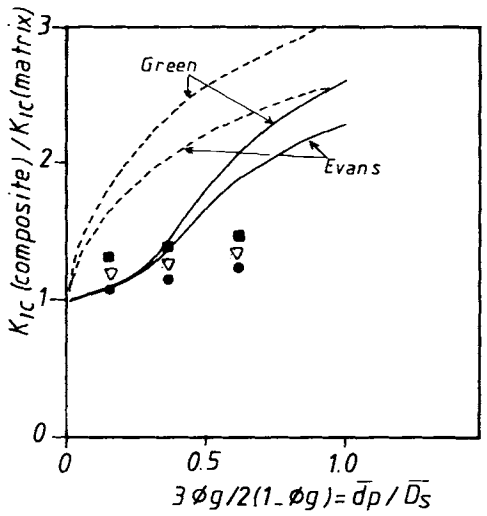

Figure 9 Comparison of experimental data and fracture mechanics theories: (-----) no-interactions and (——) interactions of secondary microcracks (same symbols as in Fig. 1).

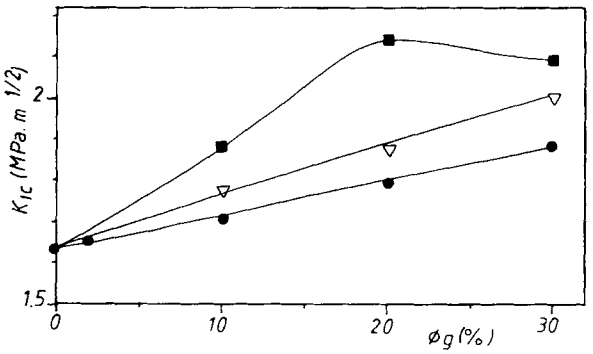

Figure 10 Stress intensity factor, K_{Ic}, as a function of vol fraction of glass beads (same symbols as in Fig. 1).

The silane treatment leads to a similar linear relationship between K_{Ic} and ϕ_g. Yet for the same volume fraction, the critical stress intensity factor is slightly lower than for untreated glass beads composites (Table III). These results are confirmed by Broutman and Sahu[4] and are contrary to the works done by Moloney et al.[49,54] and Spanoudakis,[7] who found no clear evidence on the effect of the surface treatment on the fracture properties. These authors observed an important involvement in the fracture energy for composites, based on particles treated with a release agent. This effect could be attributed to the decohesion at the glass beads surface, which favors the crack-blunting mechanism.

Contrary to this, for the coated glass beads composites, a maximum is obtained for K_{Ic} vs. ϕ_g (Fig. 10). This result is similar to those obtained by Kausch[3] on hybrid composites, for which the elastomer is dispersed in the epoxy matrix. In this case, the fractured surfaces showed many microcracks (Fig. 8), which result from the shear yielding of the epoxy matrix.[40] The size of the plastic zone, r_p, at the crack-tip as function of the volume fraction of particles is computed from the Irwin relation:[31]

$$r_p = (1/6\pi)(K_{Ic}/\sigma_y)^2$$

The values for r_p are reported in Figure 11 for the various surface treatments of glass beads. As expected, the composites based on coated glass particles display the largest plastic zones leading to a dissipation of energy by the shear yielding of the matrix.

As demonstrated in Figure 12 and in a previous paper,[42] the critical stress intensity factor, K_{Ic}, and strain energy release rate, G_{Ic}, display maxima for a thickness of about 2.8% of the particle radius. The maximum could be correlated to the decrease for

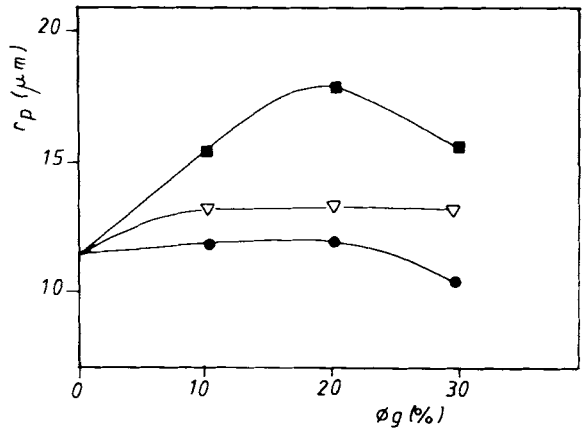

Figure 11 Plastic zone size, r_p, vs. the vol fraction of glass beads (same symbols as in Fig. 1).

the same thickness of the ratio K/M (work hardening rate-to-compression modulus). For this thickness, a greater ability to deform plastically is observed in agreement with theoretical models.[17,18] Experimental evidence of an optimum for the elastomeric interlayer was offered by Peiffer[24] and Lin et al.[46] They found a maximum of notched Izod impact strength for a thickness of about 6% on short glass fibers reinforcing an epoxy matrix. The difference in the assumptions of theoretical models (see above) and in the shape of fillers does not permit any quantitative comparison. Nevertheless, this work demonstrates that toughening could be obtained on the glass beads-filled epoxy by coating the particles with a thin layer of a crosslinked elastomer. In addition, for improvement it was necessary to control the thickness of this soft interlayer.

CONCLUSION

In this work, we have shown the effect of different parameters, such as volume fraction surface treatments of glass and thickness of an elastomeric interlayer, on the mechanical properties of glass beads epoxy composites.

As the volume fraction of glass particles increases, the Young's modulus increases, as described by various theoretical models. The nucleation and the propagation of defects, described by a metallurgical approach, decreases when ϕ_g increases. This effect could be explained by the more probable interactions between triaxial stresses around particles, as the interparticle distance decreases. The effect of glass volume fraction on the fracture properties depends on this type of test. The impact strength seems to decrease with ϕ_g and, on the contrary, an increase in crack propagation behavior is observed, which confirms the influence of the crack-pinning mechanism by rigid particles.

The stress transfer between the glass particle and the epoxy matrix is enhanced by using the γ-aminopropyltriethoxysilane as coupling agent. As a result, the interactions between stress fields around particles increase, acting against the nucleation and the propagation of defects by shearing. Thus, a higher yield stress is observed. In addition, a higher Charpy impact strength results from increasing the initiation energy of cracks.

The coating of glass beads with a thin layer of a crosslinked elastomer slightly affects the modulus of the composites and greatly enhances the fracture properties in comparison with untreated glass beads composites. This effect is attributed to the changes

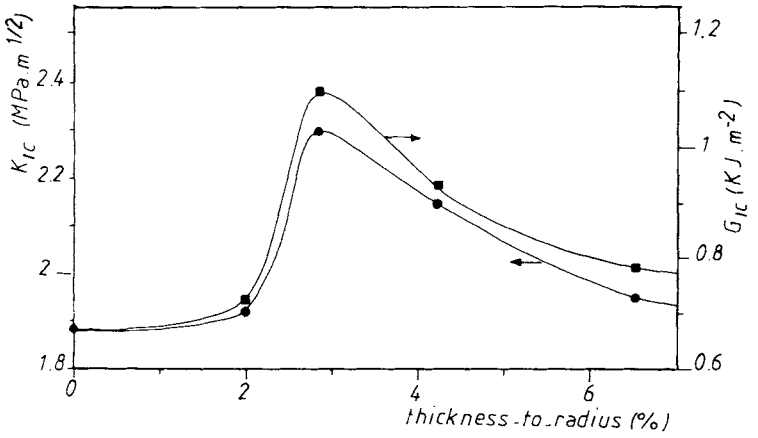

Figure 12 K_{Ic} and G_{Ic} vs. the elastomeric interlayer thickness e/r for composite based on 20% vol fraction of coated glass beads (same symbols as in Fig. 1).

in the distribution of stresses around particles, according to the micromechanical models developed in the literature.

The study of the effect of the interlayer thickness on the mechanical properties also confirms the conclusions of the theoretical models. Especially, the preyielding properties show that the thickness of the interphase influences the initiation mechanisms. Over a thickness about 2.8% of the radius of the particles, a change is observed in preplastic behavior and for the same thickness, a maximum in fracture properties is displayed. The differences between the assumption of the theoretical models and the experimental conditions do not permit a direct comparison.

In conclusion, the localization of an interphase with controlled properties (thickness and modulus, i.e., glass transition temperature) could lead to an improvement in the impact and the fracture properties without lowering the elastic properties. Such an effect could be possible by the modification of the mechanisms of initiation and propagation of the shear yielding in the epoxy matrix. Works are now in progress to study these composites in a fatigue mode using different kinds of elastomeric coatings.

We would like to thank Dr. J. M. Lefebvre for his contribution to K factor measurements. The help of G. Reffo, for the mechanical tests, was also greatly appreciated.

REFERENCES

1. R. J. Young, in *Structural Adhesives,* A. J. Kinloch, Ed., Elsevier, New York, 1986, p. 163.
2. A. C. Moloney, H. H. Kausch, T. Kaiser, and H. R. Beer, *J. Mater. Sci.,* **22,** 381 (1981).
3. A. C. Roulin-Moloney, W. J. Cantwell, and H. H. Kausch, *Polym. Comp.,* **8**(5), 314 (1987).
4. L. J. Broutman and S. Sahu, *Mater. Sci. Engn.,* **8,** 98 (1971).
5. S. Sahu and L. J. Broutman, *Polym. Engn. Sci.,* **12**(2), 91 (1972).
6. J. Spanoudakis and R. J. Young, *J. Mater. Sci.,* **19,** 473 (1984).
7. J. Spanoudakis and R. J. Young, *J. Mater. Sci.,* **19,** 487 (1984).
8. N. Sultan and F. J. McGarry, *Polym. Engn. Sci.,* **13,** 29 (1979).
9. A. J. Kinloch, D. L. Maxwell, and R. J. Young, *J. Mater. Sci.,* **20,** 4169 (1985).
10. A. J. Young, D. L. Maxwell, and A. J. Kinloch, *J. Mater. Sci.,* **21,** 380 (1986).
11. D. L. Maxwell, R. J. Young, and A. J. Kinloch, *J. Mater. Sci. Lett.,* **3,** 9 (1984).
12. A. Maazouz, N. Amdouni, H. Sautereau, and J. F. Gérard, *Proc. of JNC7/AMAC,* J. P. Favre and D. Valentin, Eds., Paris, 1990, p. 93.
13. V. A. Matonis and N. C. Small, *Polym. Engn. Sci.,* **9**(2), 90 (1969).
14. J. F. Gérard, *Polym. Engn. Sci.,* **28**(9), 568 (1988).
15. N. Amdouni, H. Sautereau, and J. F. Gérard, *J. Appl. Polym. Sci.,* to appear.
16. L. J. Broutman and B. D. Agarwal, *Polym. Engn. Sci.,* **14**(8), 581 (1974).
17. T. Ricco, A. Pavan, and F. Danusso, *Polym. Engng. Sci.,* **18**(10), 774 (1978).
18. T. Ricco and F. Danusso, *Polymer,* **20,** 367 (1979).
19. A. T. DiBenedetto and L. Nicolais, *Interfaces in Composites,* in Advances in Composite Materials, G. Piatti, Ed., Applied Science, London, 1978, p. 153.
20. M. E. T. Dekkers, J. P. M. Dortmans, and D. Heikens, *Polym. Commun.,* **26,** 145 (1985).
21. G. C. Eastmond and G. Mucciarello, *Polymer,* **23,** 164 (1982).
22. Y. G. Lin, J. P. Pascault, and H. Sautereau, in *Polymer Composites,* W. de Gruyter, Berlin, 1986, p. 373.
23. G. Riess, M. Bourdeaux, M. Brie, and G. Jouquet, in *Proceedings of the 2nd Carbon* Fibers Conference, Plast. Inst., London, 1974.
24. D. G. Peiffer and L. E. Nielsen, *J. Appl. Polym. Sci.,* **23,** 2253 (1979).
25. B. Schlund and M. Lambla, *Polym. Comp.,* **6**(4), 272 (1985).
26. J. F. Gérard, N. Amdouni, H. Sautereau, and J. P. Pascault, in *Controlled Interphases in Composite Materials,* H. Ishida, Ed., Elsevier, New York, 1990, p. 441.
27. N. Amdouni, H. Sautereau, J. F. Gérard, and J. P. Pascault, *Polymer,* **31,** 1245 (1990).
28. Y. G. Lin, J. Galy, H. Sautereau, and J. P. Pascault, in *Crosslinked Epoxies,* B. Sedlacek, Ed., W. de Gruyter, Berlin, 1987, p. 148.
29. G. Escaig, in *Plastic Deformation of Amorphous and Semi-Crystalline Materials,* B. Escaig and C. G. G'Sell, Eds., Les Ed. de Physique, Les Ullis, France, 1982, p. 187.
30. J. M. Lefebvre, C. Bultel, and B. Escaig, *J. Mater. Sci.,* **19,** 2415 (1984).
31. J. G. Williams, in *Fracture Mechanics of Polymers,* Ellis Horwood, Chichester, U.K., 1984.
32. P. K. Mallick and L. J. Broutman, *Mater. Sci. and Engn.,* **18,** 63 (1985).
33. H. Eilers, *Kolloid Z.,* 313 (1941).
34. E. H. Kerner, *Proc. Phys. Soc.,* **69B,** 808 (1956).
35. J. D. Halpin and J. L. Kardos, *Polym. Eng. Sci.,* **16,** 344 (1979).
36. O. Ishai and L. J. Cohen, *Int. J. Mech. Sci.,* **9,** 539 (1967).
37. Z. Hashin and S. Shtrickman, *J. Mech. Phys. Solids,* **11,** 127 (1963).
38. D. M. Briggs, *Polym. Composites,* **8**(2), 115 (1987).
39. J. N. Farber and R. J. Farris, *J. Appl. Polym. Sci.,* **34,** 2093 (1987).

40. O. Ishai and L. J. Cohen, *J. Comp. Mater.*, **2**(3), 302 (1968).
41. A. C. Moloney, H. H. Kausch, and H. R. Stieger, *J. Mater. Sci.*, **19,** 1125 (1984).
42. N. Amdouni, H. Sautereau, J. F. Gérard, F. Fernagut, G. Coulon, and J. M. Lefebvre, *J. Mater. Sci.*, **254,** 1435 (1990).
43. B. Turcsanyi, B. Pukanszky, and F. Tudos, *J. Mater. Sci. Lett.*, **7,** 160 (1988).
44. L. Nicolais and M. Narkis, *Polym. Eng. Sci.*, **11**(3), 194 (1971).
45. R. J. Young and P. N. R. Beaumong, *J. Mater. Sci.*, **12,** 684 (1977).
46. Y. G. Lin, J. P. Pascault, and H. Sautereau, *Annales Compos.*, **12,** 323 (1985).
47. S. K. Brown, *British Polym. J.*, **14,** 1 (1982).
48. D. G. Peiffer, *J. Appl. Polym. Sci.*, **24,** 1451 (1979).
49. A. C. Moloney, H. H. Kausch, and H. R. Stieger, *J. Mater. Sci.*, **18,** 208 (1983).
50. F. F. Lange and K. D. Radford, *J. Mater. Sci.*, **6,** 1197 (1971).
51. A. J. Kinloch and J. G. Williams, *J. Mater. Sci.*, **15,** 987 (1980).
52. A. G. Evans, *Phil. Mag.*, **26,** 1327 (1972).
53. D. J. Green, P. S. Nicholson, J. D. Embury, *J. Mater. Sci.*, **14,** 1657 (1979).
54. A. C. Moloney, H. H. Kausch, and H. R. Stieger, *J. Mater. Sci.*, **19,** 1125 (1984).

Received January 13, 1992
Accepted January 28, 1992